Journal of Inorganic Biochemistry 248 (2023) 112364

Contents lists available at ScienceDirect

Journal of Inorganic Biochemistry

journal homepage: www.elsevier.com/locate/jinorgbio

# The Cu(II) affinity constant and reactivity of Hepcidin-25, the main iron regulator in human blood

Dawid Płonka, Marta D. Wiśniewska, Joanna Ziemska-Legięcka, Marcin Grynberg, Wojciech Bal *

*Institute of Biochemistry and Biophysics, Polish Academy of Sciences, Pawińskiego 5a, Warsaw 02-106, Poland*

ARTICLE INFO

*Keywords:*
Hepcidin
Copper complex
ATCUN
Binding constant
Redox
Kinetics

ABSTRACT

Hepcidin is an iron regulatory hormone that does not bind iron directly. Instead, its mature 25-peptide form (**H25**) contains a binding site for other metals, the so-called ATCUN/NTS (amino-terminal Cu/Ni binding site). The Cu(II)-hepcidin complex was previously studied, but due to poor solubility and difficult handling of the peptide the definitive account on the binding equilibrium was not obtained reliably. In this study we performed a series of fluorescence competition experiments between **H25** and its model peptides containing the same ATCUN/NTS site and determined the Cu(II) conditional binding constant of the **CuH25** complex at pH 7.4, $^{C}K_{7.4} = 4 \pm 2 \times 10^{14}$ M$^{-1}$. This complex was found to be very inert in exchange reactions and poorly reactive in the ascorbate consumption test. The consequences of these findings for the putative role of Cu(II) interactions with **H25** are discussed.

## 1. Introduction

Hepcidin is the main iron regulator in most vertebrates. It binds to the iron exporter ferroportin (FPN) and marks it for degradation [1]. This stops the iron efflux from iron storing cells. Hepcidin is produced mainly in liver, but can be expressed also locally throughout the body in numerous tissues, including kidney and brain [2–8]. Its expression is to some extent upregulated by copper [9] and downregulated in copper deficient rodents [10,11].

In this context, the detection of full-length hepcidin (**H25**) in blood as partially bound to Cu(II) indicates a possible biological relevance of this interaction [12]. The accurate knowledge of the stability of the **CuH25** complex and its kinetic properties becomes therefore important for further assessment of its role. Tselepsis et al. attempted to determine it using Fourier-transform ion cyclotron resonance mass spectrometry (FT-ICR MS) but were able only to provide its lower limit as much <1 μM [13]. Later Kulprachakarn et al. undertook similar studies, using the native N-terminal 3-peptide (**H3**) and the N-terminal 9-peptide analog with Cys7 replaced with Ala (**H9A**) in addition to the full sequence, using potentiometry and mass spectrometry [14]. They obtained very inconsistent results. They used potentiometry to study **H3** and detected strong Cu(II) binding. We recalculated their original data using the competitivity index (CI) approach [15] and obtained the conditional affinity constant at pH 7.4, $^{C}K_{7.4}$ as $8.5 \times 10^{12}$ M$^{-1}$ for **H3**. Much lower $^{C}K_{7.4}$ values were obtained by MALDI-MS [14]: $6.3 \times 10^{8}$ M$^{-1}$ for **H9A** and 5–$6.3 \times 10^{7}$ M$^{-1}$ for the mature oxidized hepcidin-25 containing four disulfide bonds (**H25**). Such discrepancy of more than five orders of magnitude must obviously be due to a gross systematic error. We recently researched the sources of systematic errors in determinations of affinity constants of Cu(II)-peptide complexes in Electrospray Ionisation Mass Spectrometry (ESI-MS) technique. We found that systematically lower $^{C}K_{7.4}$ values reported by ESI-MS stem from the events accompanying the sample transition to gas phase [16]. The analogous process occurs in MALDI-MS. Therefore we tend to ascribe the discrepantly low affinities for **CuH9A** and **CuH25** reported in [14] to the inadequate methodology.

*Abbreviations:* ACN, acetonitrile; ATCUN, Amino-Terminal Cu and Ni binding site (containing His at position 3); α2M, α2-macroglobulin; CP, Ceruloplasmin; DMF, *N*,*N*-dimethylformamide; DMT1, divalent metal transporter protein; FPN1, ferroportin 1 protein; FT-ICR MS, Fourier-Transform Ion Cyclotron Resonance Mass Spectrometry; H25, hepcidin-25 protein; H3, peptide DTH-$NH_2$; H6, peptide DTHFPI-$NH_2$; H7W, peptide DTHFPIW-$NH_2$; H9A, peptide DTHFPIAIF-$NH_2$; hCTR1, human Copper Transporter Protein 1; HSA, Human Serum Albumin; MALDI-MS, Matrix-Assisted Laser Desorption/Ionisation Mass Spectrometry; NTS, N-Terminal Site (for Cu and Ni ions, see ATCUN); ESI-MS, Electrospray Ionisation Mass Spectrometry; TFA, trifluoroacetic acid; TIS, triisopropylsilane; EDT, 1,2-Ethanedithiol.

* Corresponding author.
*E-mail address:* wbal@ibb.waw.pl (W. Bal).

https://doi.org/10.1016/j.jinorgbio.2023.112364
Received 11 July 2023; Received in revised form 21 August 2023; Accepted 1 September 2023
Available online 2 September 2023

The Amino-Terminal Cu and Ni binding (ATCUN) family, alternatively called N-Terminal Site (NTS) family, is defined by a free N-terminal amine, any amino acid except of Pro at position two and His at position 3 [17]. The Cu(II) binding to ATCUN/NTS results in a formation of a characteristic square-planar complex defined by the coordination of the said N-terminal amine, the first two peptide nitrogens and the imidazole ring nitrogen, to complete a set of three fused coordination rings. Such sites are present in a number of human extracellular proteins and peptides, including the hCTR1 copper transporter, endostatin, histatins, human protamine 2 and some neuropeptides, where they were shown to bind Cu(II) ions. [18–23]. The ATCUN/NTS motifs are also present in many other human proteins, which remain largely uncharacterized in terms of copper physiology [24]. Except of HSA, and perhaps histatin-5 [25] and brain peptides $A\beta_{4-40,42}$ [26], the relevance of the Cu(II) complex formation for physiology of these proteins/peptides remains to be demonstrated. The large body of quantitative data for Cu(II) complexes of ATCUN/NTS peptides sets the range of their ${}^{C}K_{7.4}$ values as $10^{12}$ $M^{-1}$ to $10^{15}$ $M^{-1}$ [17].

Copper is an essential, but also a very reactive microelement. Therefore, it has to be tightly regulated on its way from the digestive tract to target enzymes in tissues. Copper trafficking in blood is a key step in this process but remains a largely unresolved issue. According to several reports reviewed by Kardos et al., the total concentration of copper in blood serum of a healthy person is slightly below 1 μg/ml, which corresponds to ca. 15 μM [27]. The majority, ca. 50–70% is contained in ceruloplasmin (CP), a ferroxidase involved in iron metabolism. The CP copper is not exchangeable in circulation, as the Cu ions are buried deep inside the folded protein and are only released at the cell surface [28,29]. Several other proteins have been proposed to carry exchangeable Cu(II) ions. Human serum albumin (HSA), the most abundant blood serum protein, has a dedicated Cu(II) ATCUN/NTS site with the occupancy of about 2–3 μM of Cu(II) (0.3–0.5% of total blood HSA) [30,31], although a higher value was also reported: 4.2 μM of Cu (II) (0.65% of total blood HSA) [28]. α2-macroglobulin (α2M) was indicated as another important copper-carrying protein at about 2 μM copper load [32], but this observation was recently contested as another study found no Cu(II) bound to α2M [28]. Hemopexin was also proposed recently to be a relevant copper-carrying protein, but its binding properties remain to be established [33]. However, all authors agree that there is a significant fraction of copper which is bound to smaller molecules (<30 kDa) in blood. It is sometimes called "free" copper although it is worth noting that no such thing as free $Cu^{2+}$ ions circulating in blood. According to various sources this low molecular weight copper pool can vary from 0.4 to 1.57 μM, depending probably on the method of detection used and on the age of test participants (this copper pool apparently decreases with age) [31,34–37].

The verified ${}^{C}K_{7.4}$ value for the Cu(II) ATCUN/NTS complex of HSA is $1 \times 10^{13}$ $M^{-1}$ at pH 7.4 [38]. Assuming that the ratio of Cu(II) loads of HSA vs α2M is 1.25 [32] and the HSA concentration is ca. 40–50 times higher than that of α2M (counting per α2M monomer) [39], the conditional stability constant at pH 7.4 (${}^{C}K_{7.4}$) of the putative α2M binding site would have to be 30–40 times higher than that of HSA, that is 3–4 × $10^{14}$ $M^{-1}$ at pH 7.4. Interestingly, no structural proposal for such site was made for α2M. The only direct evidence for Cu(II) binding to α2M comes from EPR spectra of chromatographic fractions, which were distinctly different from the ATCUN/NTS spectra. Their parameters suggested a three-nitrogen/one oxygen coordination site [40].

Divalent metals have some similar properties and biological machinery not always can distinguish among them. In particular, copper and iron homeostasis are intertwined on many levels. Iron transporter DMT1 can transport Cu(II) ions under certain circumstances [41,42]. Ferric oxidases including CP are copper proteins. The expression of ATP7A, the transmembrane copper transporter in enterocytes is strongly upregulated by iron depletion [43]. Tissue copper level was reduced in flatiron (ferroportin 1 (FPN1) mutant) mice, suggesting that FPN1 could transport copper [44]. **H25** is a direct partner of FPN1, which might be a yet another such point of cross-influence.

Recently, we demonstrated by potentiometry and spectroscopic studies that the N-terminal 6-peptide of hepcidin, DTHFPI-$NH_2$ (**H6**) binds Cu(II) with extremely high affinity, ${}^{C}K_{7.4} = 4.6 \times 10^{14}$ $M^{-1}$ which is the highest value reported so far for Cu(II) complexes with natural ATCUN/NTS sequences. We also showed that **H6** can compete Cu(II) from HSA relatively fast [45]. The high stability of this complex is further supported by the fact that it was resistant to collision induced dissociation in the MS instrument [46]. However, the accurate affinity constant is needed for the native **H25** in order to reliably assess the biological relevance of the studied interaction.

Extrapolating the ${}^{C}K_{7.4}$ values for the long ATCUN/NTS peptides/proteins from their C-terminally truncated analogs is generally not reliable [47]. The direct potentiometric approach that was employed for **H6** is not feasible since **H25** aggregates and precipitates at millimolar concentrations required by potentiometric protocols [48]. For the same reason it was not possible to perform competition experiments employing a direct detection of *d-d* bands of Cu(II) complexes, as was used for the H6 competition with HSA [45]. Instead, we developed a fluorimetric assay. We synthesized the DTHFPIW-$NH_2$ (**H7W**) peptide as a fluorescent Cu(II) competitor. We used the same sequence as in **H6** to assure the effectiveness of competition experiments by the expected similar Cu(II) affinities of both peptides. We then used the competition between **H6** and **H7W** to determine the Cu(II) affinity of the latter in the fluorescence assay and confirmed this affinity using potentiometric titrations. **H7W** was used next to determine the Cu(II) affinity of **H25**. The ROS production by redox activity of CuH25 was recently cited as mechanism of antibiotic activity of **H25** [49]. For this reason, we also investigated the ability of the Cu**H25** complex to consume ascorbate. The results are presented below.

## 2. Materials and methods

### 2.1. Materials

Amino acid building blocks for Fmoc solid phase synthesis were purchased from Iris Biotech (Marktredwitz, DE), *N*,*N*-dimethylformamide (DMF) was from Carl Roth (Karlsruhe, DE). Trifluoroacetic acid (TFA), triisopropyl silane (TIS), ethanedithiol (EDT), HEPES, HSA, ascorbic acid and EDTA were purchased from Merck (Darmstadt, DE). Diethyl ether and methanol were purchased from ChemPur (Pierkary Śląskie, PL). Acetonitrile (ACN) was purchased from Avantor Performance Materials Poland (Gliwice, PL). Clear-Ox resin was obtained from Peptides International (Louisville, KY, USA).

### 2.2. Peptide synthesis and derivatization

**H25** and its analogs, **H6** and **H7W** were synthesized using standard solid-phase peptide synthesis [50]. Cleavage of **H25** was achieved by incubation of the resin with TFA/$H_2O$/thioanisole/phenol/EDT 82.5:5:5:5:2.5 (*v*/v) for 3 h. All other peptides were cleaved by TFA/$H_2O$/TIS 95:2.5:2.5 (v/v) for 3 h. Oxidative folding of **H25** was achieved using Clear-Ox resin from Peptides International, according to the procedure described previously [51]. The formation of S-S bonds was monitored using ESI-QToF MS Premier (Waters) (Fig. S1) and visually due to different coloring of the resin (orange during the oxidation reaction and yellow after the reaction completion). Sequences of all peptides are presented in Table 1.

### 2.3. Peptide purification

**H6** and **H7W** peptides were dissolved in pure $H_2O$ and purified on RP-HPLC using the Ascentis RP-Amide 250 × 10 mm column (Sigma-Aldrich), in the $H_2O$:Acetonitrile gradient 5–40% ACN over 70 min. **H25** was dissolved in 5% acetic acid and purified on RP-HPLC using column C18-PFP 250 × 7.75 mm (ACE) in the $H_2O$:Acetonitrile gradient 25–50%

**Table 1**
Sequences of hepcidin-25 and its analogs used or discussed in this study.

| Label | Sequence |
|---|---|
| **H25** | DTHFPICIFCCGCCHRSKCGMCCKT[a] |
| **H9A** | DTHFPIAIF-amide |
| **H7W** | DTHFPIW-amide |
| **H6** | DTHFPI-amide |
| **H3** | DTH-amide |

[a] The disulfide bonds pattern is: Cys7-Cys23, Cys11-Cys19, Cys10-Cys13 and Cys14-Cys22 [52].

ACN over 50 min. TFA was a counterion in all purifications and final peptide products. It was not exchanged for competition experiments. The purity of all peptides was confirmed on ESI-QToF MS Premier (Waters). Fig. S2 presents the chromatogram of H25 after the disulfide bond formation procedure.

### 2.4. Potentiometry

Potentiometric titrations of the **H7W** peptide were performed on a Titrando 907 automatic titrator, using Biotrode electrode (Metrohm), which was calibrated daily by nitric acid titrations [53]. 0.1 M NaOH (carbon dioxide free) was used as titrant. Sample volumes of 1.2–1.5 ml were used. The samples contained 0.5 mM peptide, dissolved in 4 mM $HNO_3$/96 mM $KNO_3$. The Cu(II) complex formation was studied for the 1:1 stoichiometry using a 5–10% excess of peptide over Cu(II). All experiments were performed under argon at 25 °C, in the pH range of 2.7–10.8. The collected data were analyzed using the SUPERQUAD and HYPERQUAD programs [53,54]. Two titrations were included simultaneously into calculations, separately for protonation and Cu(II) complexation.

### 2.5. Fluorimetry

The competition experiments monitored using fluorescence were recorded on a Cary Eclipse (Varian) spectropolarimeter in 50 mM HEPES ($I$ = 0.1 M) pH = 7.4, according to the following order of reagent additions: peptide one, $CuCl_2$, peptide two. The fluorescence spectra were measured after the first two additions, and the time-course experiment was started immediately after the last addition to monitor the reaction over time up to 150 h. Additional titration experiments were performed using 30 s incubation times per each titration step. All fluorescence experiments were performed using excitation at 280 nm and emission at 355 nm.

### 2.6. Ascorbate consumption test

The kinetics of ascorbic acid (AA) oxidation was studied in 50 mM HEPES buffer, pH 7.4, on a Varian Cary Bio 50 spectrophotometer at the fixed wavelength of 265 nm. The stock of ascorbic acid concentration was determined using the extinction coefficient (ε) of $1.5 \times 10^4$ $M^{-1}$ $cm^{-1}$ at 265 nm [55]. In order to ascertain the activities of individual Cu(II) species, the reaction was studied for 0.8:1, 1:1, 1.6:1 and 4:1 peptide/Cu(II) ratios, using $Cu^{2+}$ ions in HEPES buffer (that is, a redox-prone Cu(HEPES) complex [56] and free peptide as a positive and negative control, respectively. The total Cu(II) concentration was 5 μM and the initial AA concentration was 100 μM in all cases. The reactants were added after the 10 min. Incubation of the AA solution and the reactions were monitored for further 30 min.

### 2.7. Generation of tree of Life for mammalian hepcidins

In order to collect protein sequences of hepcidins, the jackhammer search in UniProtKB with human hepcidin (UniProtACC: P81172) was used as input [57,58]. Proteins other than hepcidin and proteins deleted in the new version of UniProtKB (version 2023_03) were removed from the dataset [59]. Next, the information was collected about source genes from UniProtKB, only one isoform was selected per organism. Each sequence was then manually cut according to the real furin processing site. To register mutations in positions of interest, RefSeq references about mRNA were collected and regions of active hepcidin were found [60]. Finally, the ETE3 package in Python was used to show protein positions, with numbers of proteins containing a histidine in the third position marked on the Tree of Life [61].

## 3. Results

### 3.1. Solubility of H25 and choice of methodology

The mature hepcidin, **H25** as well as its Cu(II) complex are poorly soluble in water. Its solution structure was determined previously in a phosphate-buffered solution, which improved the solubility [62]. However, buffering precluded the use of potentiometry to study the strength of Cu(II) binding to **H25.** Preliminary attempts to perform spectroscopic titrations based on the Cu(II)-related chromophore (*d-d* and charge-transfer absorption bands) indicated the peptide aggregation, apparently not detected in the published NMR study [62]. Calorimetry and microscale thermophoresis (MST) could not be used, because the expected complex affinity ~$10^{14}$ $M^{-1}$ is well beyond the range available to these methods [63,64]. Fluorescence spectroscopy remained as the only readily available technique with sufficient sensitivity to detect changes in complexes at micromolar concentrations of peptides. This, however, depended on the presence of a suitable fluorophore. For this purpose, we chose to synthesize the **H7W** peptide (Table 1). **H7W** is the closest possible analog of **H6** in terms of Cu(II) binding, while the addition of the Trp fluorophore at position seven was considered distant enough from the ATCUN/NTS site to limit the interference with the Cu(II) binding mode, but close enough to remain susceptible to quenching by the Cu(II) ion coordinated at the ATCUN/NTS site. These notions were based on a previous study of the Tyr quenching by Cu(II) coordination to the $A\beta_{4-16}$ peptide in which the Tyr residue was also at position seven from the N-terminus containing the ATCUN/NTS motif [65].

### 3.2. Validation of H7W as Cu(II) competitor for fluorescence detection

In the first experiment we investigated the effect of Cu(II) binding on Trp fluorescence in **H7W**. As presented in Fig. 1, the fluorescence emission signal was quenched by Cu(II) complexation by up to 50%, with a linear relationship between the fluorescence intensity and the molar fraction of the complex. The fluorescence maximum at 355 nm was not shifted by complexation. Further fluorescence decrease was caused by incremental dilution of the sample by the titrant $CuCl_2$ solution. Therefore, the fluorescence signal at 355 nm could be used to monitor the Cu(II) binding to **H7W** in competition experiments.

Next, competition experiments between **H6** and **H7W** were performed. Preliminary experiments indicated that the Cu(II) exchange between these two peptides was slow. Therefore, the progress of reaction was monitored for four days (Fig. 2). The reaction equilibrium was achieved after ~90 h. Two modes of experiment were used. In one the pre-formed **CuH6** complex (10 μM) was mixed with the equimolar **H7W**, and in another the 10 μM **CuH7W** complex was mixed with the equimolar **H6**. As seen in Fig. 2, very similar final fluorescence intensities were reached in these independent experiments. The Trp fluorescence could, however, be quenched by two mechanisms. In addition to static quenching by Cu(II) binding to **H7W**, dynamic quenching by the fluorophore collisions with paramagnetic Cu(II) complexes could be effective. In order to investigate this possibility, we performed partial titrations of 10 μM **H7W** with **CuH6** with short incubation times, about 1 min. The extent of Cu(II) exchange between these peptides was

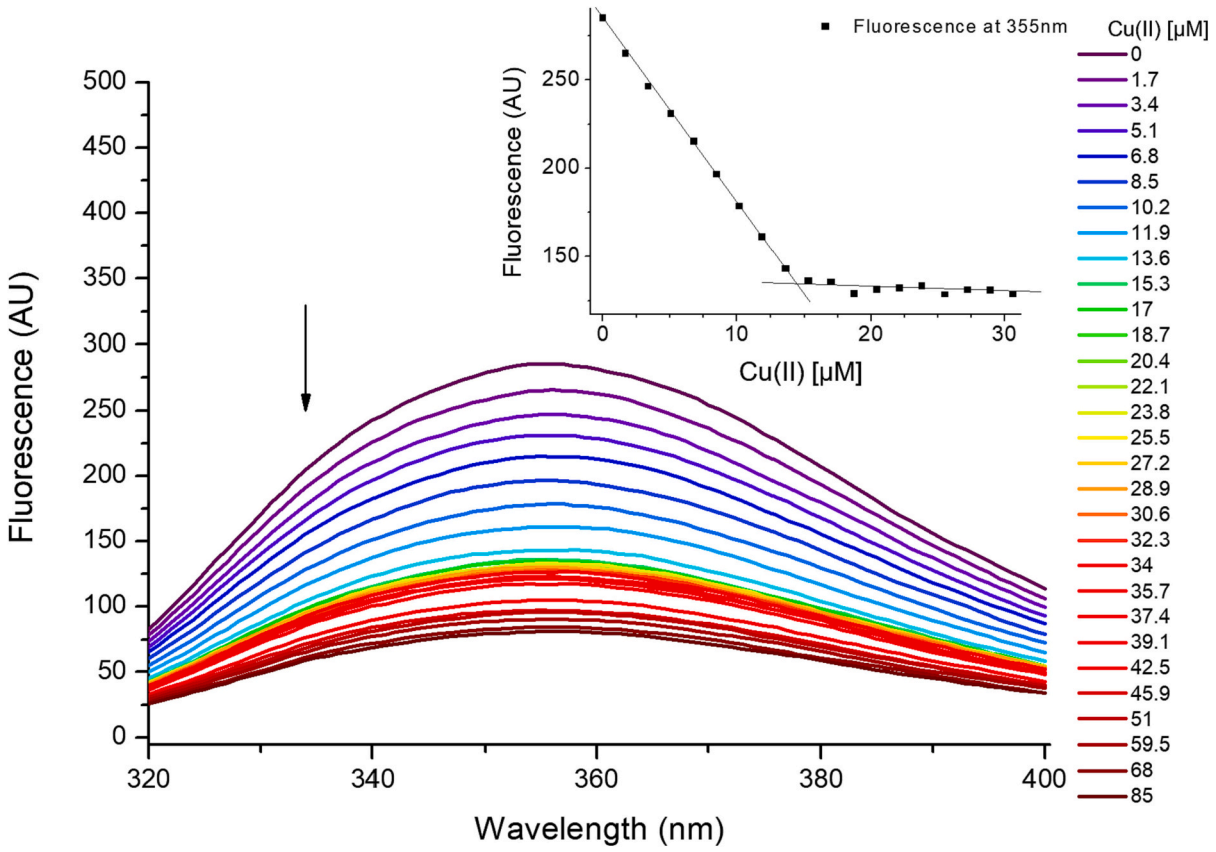


**Fig. 1.** Quenching of fluorescence of 14.5 μM DTHFPIW-$NH_2$ peptide (**H7W**) by increasing μM concentrations of Cu(II) ions (indicated on the plot). The excitation wavelength was 280 nm. Inset shows the emission intensity changes at 355 nm.

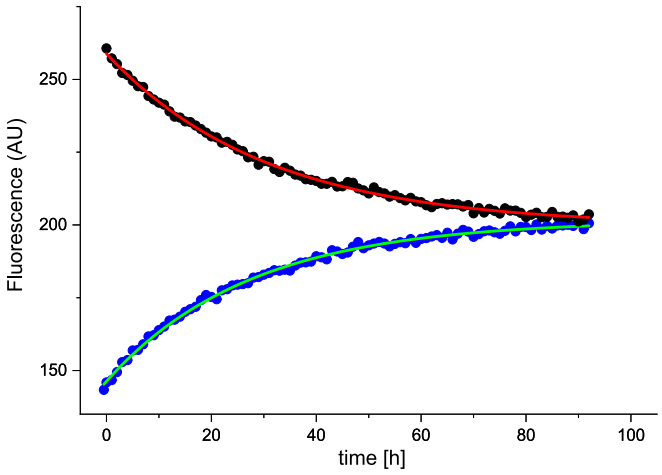


**Fig. 2.** Evolution of Trp fluorescence in Cu(II) competition experiments between **H6** and **H7W** peptides monitored by emission at 355 nm: 10 μM **H7W** + 10 μM **CuH6** (black dots); 10 μM **CuH7W** + 10 μM **H6** (blue dots); and 1st order kinetic fits (red and green lines, respectively). (For interpretation of the references to colour in this figure legend, the reader is referred to the web version of this article.)

negligible at such times, which empowered us to generate a titration curve describing the dynamic quenching process (Fig. 3). The extent of quenching was 11% for 10 μM **CuH6** (beginning of the **H7W** + **CuH6** reaction), down to 6% for 5 μM **CuH6** (roughly corresponding to the reaction endpoint). These small effects did not affect the shape of first order exchange kinetics in the competition experiment. Therefore, we could use the kinetic experiments to determine the ${}^{C}K$ values at pH 7.4 for **CuH7W** (${}^{C}K_{CuH7W}$, formally defined by Eq. (1)), using the known constant for **CuH6** (${}^{C}K_{CuH6}$, Eq. (2)) [45], and the experimental derivation of the equilibrium constant of the Cu(II) competition reactions, $K_{eq}$, defined by Eq. (3), to obtain the numeric value of ${}^{C}K_{CuH7W}$ from Eq. (4). In these eqs. [H6], [CuH6], [H7W] and [CuH7W] represent all protonation forms of the respective peptides and complexes at pH 7.4.

$$ {}^{C}K_{CuH7W} = [CuH7W]/([Cu^{2+}] \times [H7W]) \quad (1) $$

$$ {}^{C}K_{CuH6} = [CuH6]/([Cu^{2+}] \times [H6]) \quad (2) $$

$$ K_{eq} = {}^{C}K_{CuH7W}/{}^{C}K_{CuH6} = ([CuH7W] \times [H6])/([Cu^{2+}] \times ([CuH6 \times [H7W]) \quad (3) $$

$$ {}^{C}K_{CuH7W} = {}^{C}K_{CuH6} \times K_{eq} \quad (4) $$

The equilibrium values of [CuH7W] and [H7W] were obtained from the fitted kinetic curves, using the fluorescence intensities of **H7W** and **CuH7W**, obtained from the calibration experiment presented in Fig. 1, and corrected for the dynamic quenching according to Fig. 3. The kinetic parameters and ${}^{C}K_{CuH7W}$ values (Eq. (4)) are presented in Table 2. The average ${}^{C}K_{CuH7W}$ value, $5.3 \pm 0.7 \times 10^{14}\ M^{-1}$ (log value $14.72 \pm 0.06$) is not significantly different from the value of ${}^{C}K_{CuH6}$ ($4.6 \pm 0.5 \times 10^{14}\ M^{-1}$, log value $14.66 \pm 0.05$).

### 3.3. Competition for Cu(II) between H25 and H7W peptides

The validation of the fluorescent **H7W** peptide as a Cu(II) chelator suitable for competition experiments with other hepcidin peptides empowered us to perform them for **H25**. An example of such set of experiments, which included two complementary exchange reactions (**H7W** + **CuH25** ⇔ **CuH7W** + **H25** and **CuH7W** + **H25** ⇔ **H7W** +

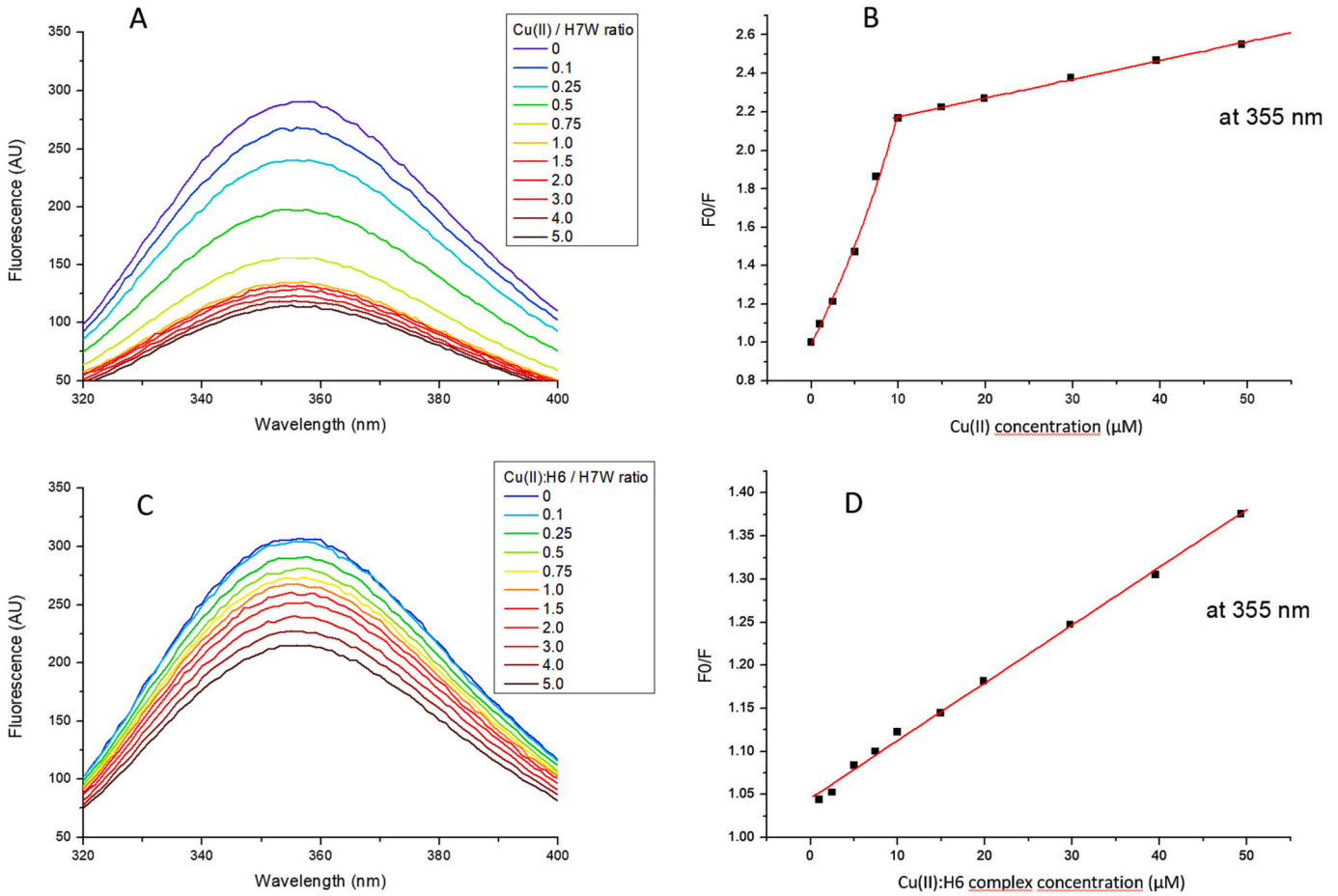


**Fig. 3.** 10 μM **H7W** fluorescence quenched by titration with Cu(II) (A, B) and Cu(II):**H6** 1:1 complex (C, D) monitored by emission at 355 nm, $\lambda_{ex}$ = 280 nm: A, C are raw spectra; B, D are Stern-Volmer plots of respective reactions.

**Table 2**
Kinetic and thermodynamic parameters of Cu(II) competition reactions between the **H6** and **H7W** peptides. Statistical errors on the last significant digits are given in parentheses.

| Reaction | Reaction half-time (h) | $K_{eq}$ | ${}^{C}K_{CuH7W}$ | Log ${}^{C}K_{7.4}$ |
|---|---|---|---|---|
| **CuH7W** + **H6** | 19.0(3) | 1.00 (1) | $4.60(5) \times 10^{14}$ $M^{-1}$ | 14.67(1) |
| **CuH6** + **H7W** | 21.2(2) | 1.32 (6) | $6.1(2) \times 10^{14}$ $M^{-1}$ | 14.78(2) |
| Average | | | | 14.72(6) |

**CuH25**) and two control incubations (**H7W** and **CuH7W**) is presented in Fig. 4. Other reaction sets are provided in Fig. S3. In all reactions the kinetic curves were monoexponential, corresponding well to the pseudo-1st order rate law.

The rate of Cu(II) transfer from **H7W** to **H25** (black symbols in Figs. 4 and S3) was concentration dependent. The reaction half-times ($t_{½}$) of ca. 18 h and 12.5 h for ~5 μM and ~ 10 μM reactants, respectively, were shorter than that for the Cu(II) transfer from **H7W** to **H6,** ca. 19 h. The reverse reaction t½ (red symbols) were much slower in all cases and did not reach equilibrium even after 10 days of incubation. The reaction endpoints had to be extrapolated instead. The obtained $t_{½}$ values varied between 23.3 ± 0.3 and 99 ± 3 h, in all cases being higher than that observed for the Cu(II) transfer from **H6** to **H7W,** 21.2 ± 0.4 h.

The results of the equilibrium constant calculations based on all eight independent experiments are presented in Table 3, while the underlying kinetic curve fit parameters are given in Table S1. The $K'_{eq}$ values presented in Table 3 were obtained according to Eqs. (1 and 5). The average of these determinations was used to obtain the value of ${}^{C}K_{CuH25}$ according to Eq. (6). The average value calculated for all experiments and that for only the lower concentration experiments are provided.

$$K'_{eq} = {}^{C}K_{CuH7W} / {}^{C}K_{CuH25} = ([CuH7W] \times [H25]) / ([Cu^{2+}] \times ([CuH25] \times [H7W])) \quad (5)$$

$${}^{C}K_{CuH25} = {}^{C}K_{CuH7W} / K'_{eq} \quad (6)$$

In experiments starting from **CuH7W** and **H25** the sample fluorescence increased due to the liberation of more strongly fluorescent **H7W** by formation of **CuH25**. In reverse experiments the sample fluorescence decreased due to the quenching of **H7W** fluorescence upon the Cu(II) interception from **CuH25**. In equimolar systems, such as experiments 2, 3 and 4 described in Tables 3 and S1 these two effects should add up to match the difference between the initial fluorescence of the corresponding **CuH7W** and **H7W** samples. This was the case for the **H7W**/**H6** couple (Fig. 2) but not for the experiments with **H25**. The deficit ranged between 13 and 21% (Fig. S3, Table S1). It could not be explained by photobleaching or dynamic scattering, because these phenomena would rather lower the overall fluorescence, but this was observed neither in competition experiments nor in controls. It seems that the Cu(II) exchange reaction was stopped before reaching equilibrium, thus accounting for the systematic discrepancies of $K'_{eq}$ values between the two experiment modes. A clue for explaining this effect may be hidden in the rates of respective reactions. The rates of Cu(II) dissociation from the **CuH7W** complex depended on both the initial complex concentration and the exchange partner, being slower for **H6**. This means that **H25**

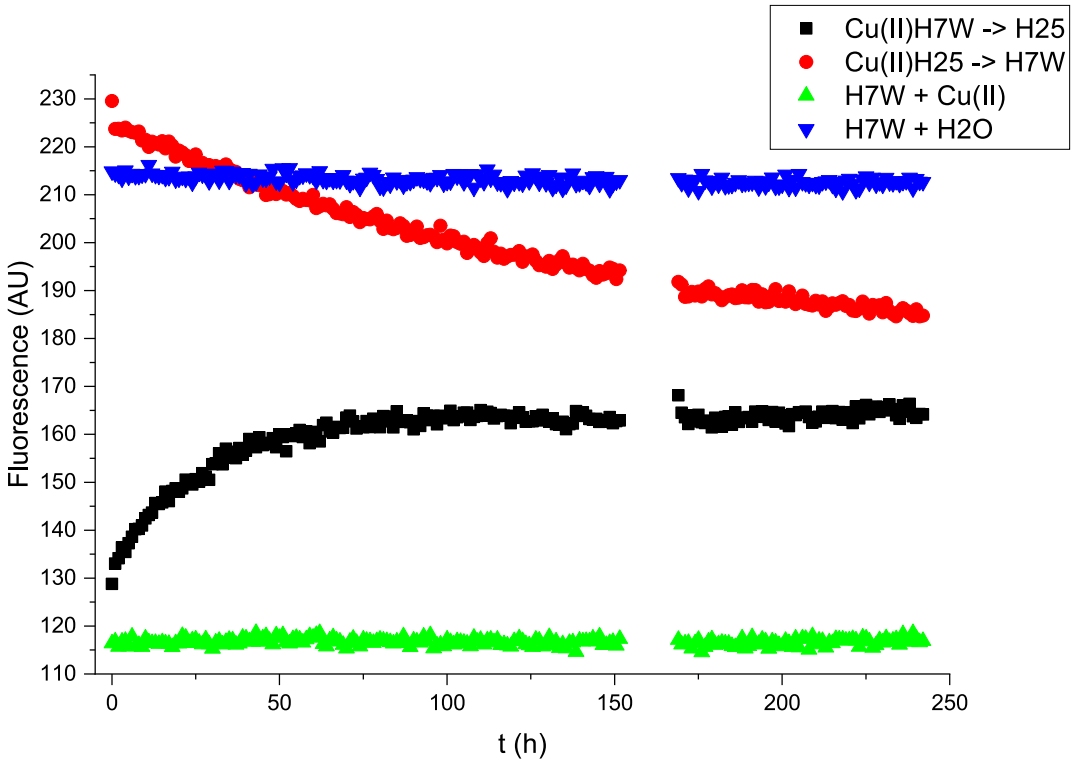


**Fig. 4.** Set 4 (Table 3) of competition experiments for Cu(II) transfer between **H7W** and **H25**. Black: 5.3 μM of **H25** was added to 5.3 μM of **CuH7W**. Red: 5.3 μM of **H7W** was added to 5.3 μM of **CuH25**. Green: control 5.3 μM **CuH7W** sample. Blue: control 5.3 μM **H7W** sample. Both controls were diluted with water to obtain the same final concentrations of reagents in all four cases. (For interpretation of the references to colour in this figure legend, the reader is referred to the web version of this article.)

**Table 3**
Equilibrium constant values for Cu(II) competition between **H7W** and **H25** peptides. Equimolar peptides were used in all four sets of experiments. $^{C}K_{CuH7W} = 5.3 \pm 0.7 \times 10^{14}$ $M^{-1}$.

| Experiment set | $K'_{eq}$ according to Eq. (5) | | Concentrations of H7W and H25 (μM) | Average log $^{C}K_{7.4}$ |
|---|---|---|---|---|
| | **CuH7W + H25** | **H7W + CuH25** | | |
| 1 | 7.13 ± 0.21 | 2.78 ± 0.19 | 8.2 / 9.2 | 14.1 ± 0.2 |
| 2 | 7.57 ± 0.39 | 1.58 ± 0.03 | 10.6 / 10.6 | 14.2 ± 0.3 |
| 3 | 3.38 ± 0.51 | 0.67 ± 0.04 | 5.4 / 5.4 | 14.5 ± 0.3 |
| 4 | 2.04 ± 0.14 | 0.74 ± 0.04 | 5.3 / 5.3 | 14.6 ± 0.2 |
| Average | 3.2 ± 2.7[a] / 1.4 ± 1.0[b] | | | 14.4 ± 0.2/ 14.6 ± 0.2 |

[a] From all experiments.
[b] From experiments performed for 5.3–5.4 μM peptides.

interacted with **CuH7W**. The reverse reaction was much slower, but very poorly reproducible in terms of the reaction rate. Together with the tendency of **H25** to aggregate, these facts suggest that co-aggregates of **CuH7W**, **H25** and **CuH25** may be formed in the course of the exchange reaction, eventually stopping it prematurely. For this reason, the reaction with **H25** performed at lower peptide concentrations may be more reliable. In additional support for the above consideration, we demonstrated that both **H25** and **CuH25** had a small, but nearly identical quenching effect towards 5.7 μM **H7W** (Fig. S4). This experiment was performed for short, 30 s sample incubation times, in order to avoid the effect of Cu(II) transfer from **CuH25** to **H7W**. As additional control, **H7W** was titrated with Cu(II) ions under the same conditions, which resulted in the expected strong and quantitative fluorescence quenching.

### 3.4. Ascorbate consumption by CuH25

The consumption of ascorbate (AA) is a facile test of oxidative capacity of Cu(II) complexes under physiological conditions, and is related to the ability of the given complex to maintain the Cu(II)/Cu(I) redox couple [66]. As seen in Fig. 5, the **CuH25** complex showed very low ascorbate consumption activity of 20 nM AA/s, about 1% of that presented by $Cu^{2+}$ ions in HEPES. Table S2 presents the individual reaction rates.

### 3.5. Potentiometric determination of Cu(II) affinity to H7W (DTHFPIW-amide)

The potentiometric titrations were aimed at validating the performed for 0.5 mM **H7W**, due to the sensitivity of the method. The obtained protonation constants and log β values for Cu(II) complexes are presented in Table S3. We used these data to calculate the $^{C}K_{7.4}$ value for **CuH7W** according to the CI methodology [15]. The obtained value was $5.2 \pm 0.7 \times 10^{13}$ $M^{-1}$, 10-fold lower from the values obtained in competition titrations for **CuH7W** and in previous validated potentiometric studies of **CuH6** [45].

### 3.6. His-3 evolutionary conservation in hepcidins

In order to place the above findings in the biological and evolutionary context we investigated the emergence of His-3 in mature hepcidins across the mammals. Most fish hepcidins perform antimicrobial function, birds seem to lack hepcidin as a mechanism of iron regulation [67] and the data for amphibians and reptiles are too scarce to draw meaningful conclusions despite all of them apparently containing His-3.

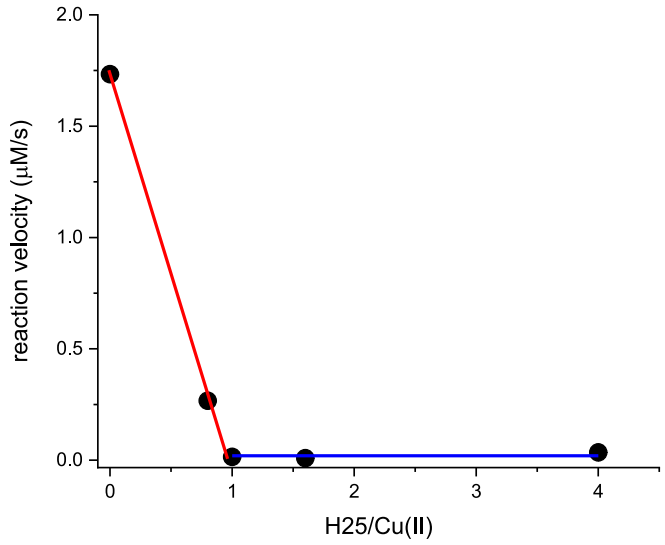


**Fig. 5.** Dependence of ascorbate oxidation rate on the **H25**/Cu(II) ratio. Upon the exposure to 5 μM Cu(II) and varying concentrations of **H25**. The reaction was monitored at 265 nm. Red line marks the linear dependence of ascorbate consumption on the amount of Cu(II) not complexed to **H25**. Blue line marks the average ascorbate consumption by the **CuH25** complex, 20 nM AA/s. (For interpretation of the references to colour in this figure legend, the reader is referred to the web version of this article.)

To facilitate the search, we assumed the propeptide cleavage site recognized by furin, canonically RXK/RR, with few exceptions. The fragment always included the cationic region ending with Arg. The search data are presented in detail in Supplementary File 2, while the presence of His-3 in hepcidins is visualized by the tree-of-life diagram in Fig. 6. One can immediately recognize that His-3 positively differentiates *Eutheria* from the evolutionarily older *Marsupia* and *Monotremata*. In the latter, it is apparently present in position 4 after the cleavage site, with an aromatic amino acid inserted directly after the cleaved Arg (alternatively the furins of these organisms could have an altered cleavage site, but there is no data on this issue). His-3 is strictly conserved in most higher mammals including all primates. There are only two types of exceptions: about the half of sequenced rodent species, including *Mus muculus* and *Rattus norvegicus* have His-3 replaced with Asn, while *Mus caroli* (Ryukyu mouse) as well as the sole sequenced hedgehog have His-3 replaced with Tyr.

## 4. Discussion

### 4.1. Cu(II) binding to H25

The prime objective of this study was to establish the **H25** affinity for Cu(II) in an unbiased fashion under conditions as close to the natural ones as possible. This included working at pH 7.4 characteristic of blood serum and using the lowest possible concentrations that allowed for reliable detection of the studied species. The latter condition was required by the natural low abundance of **H25** in blood serum and by the propensity of this peptide to aggregate at millimolar and submillimolar concentrations observed in the course of our experiments. Therefore, a stepwise procedure was applied, making use of the ability of fluorescence spectroscopy to detect and quantify micromolar amounts of the tryptophan fluorophore present in the competitor peptide. In this procedure the **H6** peptide was used as benchmark because its binding constant for Cu(II) ions was established previously with high accuracy by independent methods [45]. Then, the set of competition experiments was performed for the **H6**/**H7W** couple, where the partial quenching of the **H7W** fluorophore due to Cu(II) binding was used to report the state of equilibrium (Fig. 2). Together with the validation of proportionality of **H7W** static quenching to the fraction of Cu(II) bound to the peptide (Fig. 1) and the estimation of the contribution of dynamic quenching to the overall fluorescence of **CuH7W** (Fig. 3), the reliable value of $^{C}K_{CuH7W}$ was obtained (Table 2), which did not differ significantly from that for **CuH6**. Next, **H7W** was used in analogous Cu(II) competition experiments with **H25**. As described in the Results section and illustrated in Figs. 4 and S3 these experiments exhibited a small but systematic bias, depending on the direction of competition reaction. The log $^{C}K_{7.4}$ values from reactions in which **CuH25** was formed were on average 0.55 ± 0.15 log units lower from the reverse case. Also, comparing the fluorescence evolution in these two complementary reactions, they seemed to find different endpoints. This was not the case for the **H6**/**H7W**. Also, the log $^{C}K_{7.4}$ values for experiments performed at 10 μM concentrations yielded the log $^{C}K_{7.4}$ values 0.4 ± 0.1 log units lower than those at 5 μM. Furthermore, the equilibration processes which included dissociation of **CuH25** were slower and much less reproducible in terms of $t_{½}$ values than the reverse processes. We interpret these effects collectively as evidence for the concentration-dependent formation of **H25/CuH25** aggregates in which Cu(II) ions cannot access all **H25** molecules. In such case the higher log $^{C}K_{7.4}$ values should be the more reliable one, placing the final log $^{C}K_{7.4}$ value for **CuH25** around 14.6. This value is given in Table 4 along with the average value over all experiments. Altogether, with all the above caveats, we proved **H25** to be a very strong Cu(II) chelator, and the derived affinity constant can be used in predictions of additional biological roles of **H25.**

The analogous problem manifested itself in a potentiometric determination of **CuH7W** stability. Working at 0.5 mM concentrations we obtained the log $^{C}K_{7.4}$ value one order of magnitude lower than expected (Table 4). Upon careful inspection of titration curves we noticed a systematic worsening of the fit in the segments of titration curves corresponding to the ATCUN/NTS complex. Such effect, which can be attributed to the increased glass electrode drift, was not present in titrations of **H7W** alone. These titrations yielded protonation constants being in a fair agreement with those presented for **H6** [45] (see Table S3). We interpret these effects to be due to slow aggregation of **CuH7W** at concentrations 100 times higher from those used in fluorescence experiments. Indeed, a similar but more pronounced effect was noted in our attempts of potentiometric titrations of **CuH9A** and **CuH25**, but in both cases it resulted in a failure of stability constant calculations and in the latter case the aggregation was visible with naked eye at pH 6 and higher (data not shown). It seems that **H6** is the longest fairly soluble hepcidin peptide, and the extension of the hydrophobic patch starting at residue 4 yields an efficient template for peptide aggregation.

### 4.2. Biological relevance of high H25 affinity for Cu(II)

The tree-of-life analysis presented in Fig. 6 and Supplementary File 2 provided an interesting but unequivocal view on the appearance of His-3 in **H25** sequence of mammals, hence the relevance of Cu(II) binding ability of **H25**. We were able to find and analyze 120 sequences from 13 orders, but not all of these orders had sufficient coverage, with as few as single cases in four of them. The His-3 appears in placental animals in contrast to *Monotremata* and *Metatheria* which have a Phe residue inserted between the furin cleavage site, making the His residue present there His-4 rather than His-3. Peptides containing His-4 form much weaker Cu(II) complexes [17], which are not likely to have a biological function. We have no data on *Monotremata* and *Metatheria* propeptide convertase specificity, so it is even possible that their hepcidins have His-3 as well.

Nevertheless, the certain His-3 sequence is perfectly well conserved in most eutherian orders. However, this conservation is lost in rodents (replaced by Asn, or Tyr), where only seven out of 13 known **H25** sequences have it. This includes such scientifically important species as *Rattus norvegicus* and *Mus musculus*. His-3 is also missing (replaced by Tyr) in the only studied case of *Eulipotyphla*, the European hedgehog.

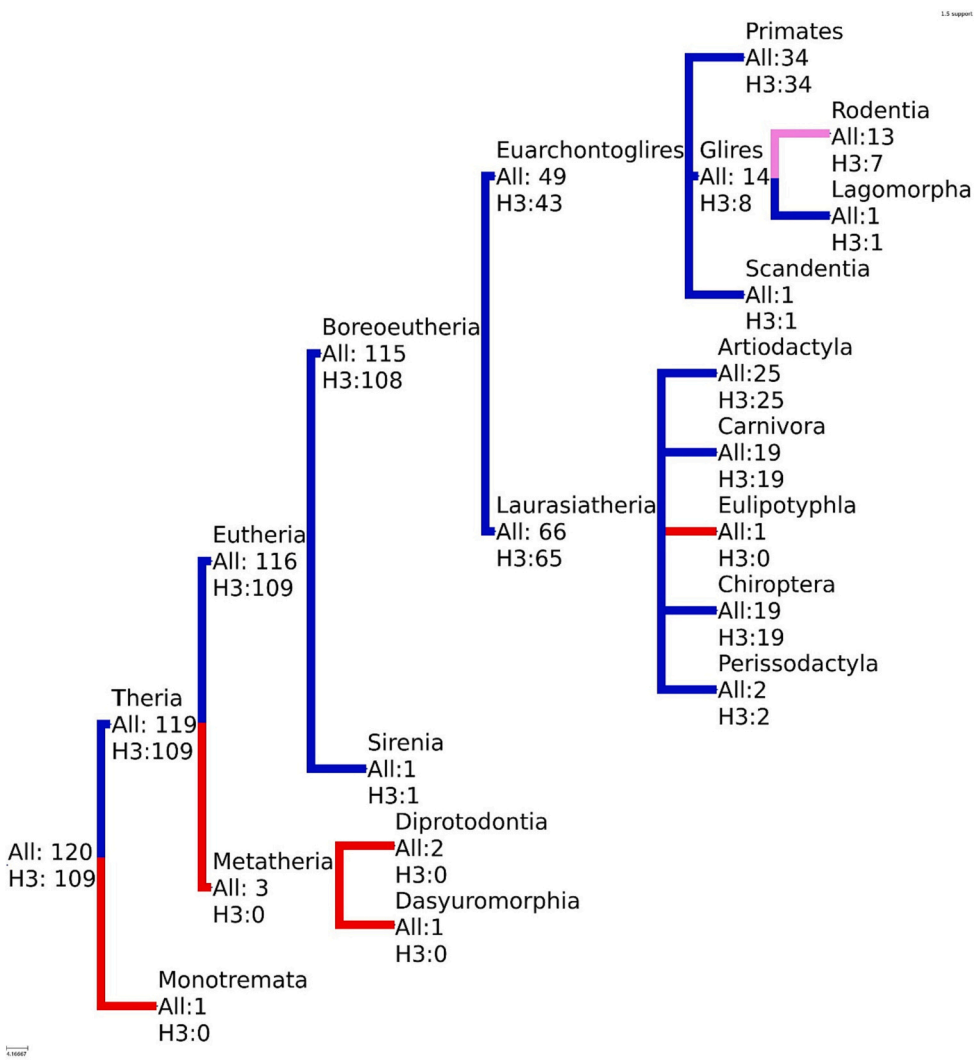


**Fig. 6.** Evolution of hepcidin in mammals tested for His 3 in mature peptide (**H25**).

**Table 4**
Copper(II) affinity constants ($^{C}K_{7.4}$ expressed logarithmically) for different hepcidin peptides and methods used to determine them. See Table 1 for peptide abbreviations.

| Peptide | Log $^{C}K_{7.4}$ | Method | Reference |
|---|---|---|---|
| H3 | 12.9 | Potentiometry and UV–vis | [14] |
| H6 | 14.66 ± 0.06 | Potentiometry and UV–vis | [45] |
| **H7W** | **14.72 ± 0.06** | **Competition** | **This work** |
| H7W | 13.72 ± 0.06 | Potentiometry | This work, unreliable due to aggregation |
| H25 | 7.8 | MALDI-MS serial dilution | [14] |
| H25 | > > 6 | FTICR-MS | [13] |
| **H25** | **14.4 ± 0.2**[a]/ **14.6 ± 0.2**[b] | **Competition** | **This work** |

[a] Average value of all determinations for 10 μM and 5 μM **H25** concentrations.
[b] Recommended value based solely on experiments for 5 μM **H25** concentrations.

These facts indicate that strong Cu(II) binding may be important for most mammals, but this function may not be indispensable, or else there is a compensatory innovation in some rodents (and hedgehogs). This way or another, the total conservation of His-3 in primates empowers us to speculate on its relevance in humans.

His-3 is one of the most important residues for hepcidin function as a ferroportin partner [68]. However, its replacement with Phe worked almost just as well, which allows us to state that Cu(II) binding cannot be essential for the iron regulatory activity. However, the Cu(II) binding was found to slightly enhance the antibacterial activity of **H25**, which depended on the correct formation of the disulfide bonds [69]. Moreover, the anticandidal activity demonstrated for **H25** apopeptide was decreased in the presence of Cu(I) chelator bathocupreinedisulfonic acid (BCS) and enhanced by co-exposure with ascorbate. The authors cited previous studies which related ATCUN/NTS model peptides with Cu(I)/Cu(II) cycling and ROS production and concluded that the binding of endogenous copper and ROS activation was responsible for this activity [49]. Indeed, slow ascorbate-induced ROS production was demonstrated, among others, by the CuDAHK complex representing the ATCUN/NTS site of HSA [66]. In ATCUN/NTS peptides this is related to the relative stability/lifetime of the intermediate 2 N complex [70]. However, we found that **CuH25** was not able to consume ascorbate effectively, which means that it would rather not be able to produce ROS under physiologic conditions. Therefore, the actual biocidal mechanism of **H25/CuH25** remains to be established. One possibility is that **H25** sequesters Cu(II) ions required for the pathogen growth. A similar mechanism was postulated previously for other antimicrobial peptides [71].

Copper distribution and transport in blood is not a completely resolved issue, and there still are many uncertainties. A sizeable portion

of blood copper is bound to ligands below the 10 kDa threshold [28]. The molecular weight of **H25** is 2789.35, well within this limit. Depending on the purification method, some of **H25** could be detected in blood as Cu(II) complex. In [46] blood serum was filtrated with a 30 kDa cut-off, followed by the enrichment of the filtrate sample with a Cu(II) salt. In such conditions 100% of hepcidin was found as **CuH25**. Even collision induced dissociation in mass spectrometer did not remove the $Cu^{2+}$ ion from the peptide. Instead, the main fragment ion was CuDTH. These data indicate that **H25** might participate in Cu(II) homeostasis.

The ${}^{C}K_{7.4}$ value determined in this work can be used to assess the putative equilibrium ratio of **CuH25** to **H25,** using the data available for HSA. The maximum **H25** blood concentration reported for a patient with inflammation was reported as 1.5 μM [72], but in healthy subjects, mean **H25** blood concentration is ~7.2 nM [73]. Taking log ${}^{C}K_{7.4}$ values of 14.6 and 13.0 for **H25** and HSA, respectively, their concentrations as 7.2 nM and 650 μM [74] and the HSA saturation with Cu(II) ions as 0.65% [28], one can quickly calculate the concentration of Cu(II) bound to **H25** as ~1.5 nM, i.e. ca. 20% of total **H25**.

On the other hand, the turnover of **H25** in blood is fast. Its half-life in blood was reported as 2.3 min in *Cynomolgus* monkeys [75]. Therefore, **CuH25** formed by sequestering Cu(II) from weaker ligands by H25 may not have time to exchange Cu(II) ions with HSA, and rather would carry Cu(II) elsewhere, upon its clearance, in an off-equilibrium fashion. As indicated above, the proteolysis of **CuH25** e.g. to **CuH6** would not decrease the Cu(II) affinity of the DTH ATCUN motif. These observations may be worthy of a further study in the context of the reported antimicrobial activity of **H25**. scavenger, diminishing copper bioavailability to infectious microbes. This would be possible, because the extremely slow rate characterizes only the ATCUN-to-ATCUN Cu(II) exchange. This, according to our other studies, is dictated by very low $k_{off}$ values for the hepcidin's ATCUN motif. The $k_{on}$ has not been determined, but the formation of **CuH25** 4 N complex may take significantly <1 s, possibly sufficiently fast to maintain for a Cu(II) scavenger role [76,77].

Upon a rigorous in vitro test, the ability of pure α2M to bind Cu(II) ions was neglected [28]. On the other hand, depending on the source, as much as 89% [78] or as low as 3% [79] of circulating **H25** can be bound to α2M. Inspired by the high stability of **CuH25**, we are prompted to speculate that α2-macroglobulin is not a Cu(II) carrier per se, but can rather carry **CuH25** and other low molecular weight Cu(II) chelators. Also, this hypothesis could be tested in carefully performed analytical and in vitro experiments. We are aware of the fact the only available data on the chemical nature of Cu(II) ions present in α2M complexes indicate the non-ATCUN/NTS structure [40], but these two points are not as contradictory as it might seem. The relative Cu(II) occupancy of α2M and HSA was obtained from a different series of experiments and a different technique [32] and α2M could as well carry other Cu(II) complexes in that case.

The inertness of **CuH25** in Cu(II) exchange reactions is another factor enhancing the likelihood of its contribution to Cu(II) blood homeostasis. Recent findings regarding kinetic properties of ATCUN/NTS complexes indicate the relevance of second-to-minute time windows in copper distribution from the intestine through blood to liver and other organs [76,77]. Under such conditions the **CuH25** complex once formed may be sufficiently long-lived to exert its hypothetical copper-related functions before being cleared from the bloodstream or exchanging the Cu(II) ion. To briefly test one such hypothetical function, we tested whether **H25** could theoretically protect against redox properties of Cu(II). In equimolar concentrations, ascorbate as a substrate was consumed slower by two orders of magnitude with the Cu(II) ion trapped in the **CuH25** complex (Fig. 5, Table S2), indeed supporting such role.

## 5. Conclusions

Hepcidin-25 was demonstrated to be a very strong chelator for Cu(II) ions, likely to be at least partially Cu(II) bound in the bloodstream. The distinct inertness of the **CuH25** complex in $Cu^{2+}$ exchange reactions suggests that the complex should be considered as a distinct entity, rather than a Cu(II) delivery agent, in analyzing its physiological role. The lack of ascorbate reactivity precludes its participation in physiological redox processes and also the redox-based toxicity. The sequence analysis revealed that the ATCUN site in mammalian hepcidins is significantly, but not universally conserved. This suggests a secondary or complementary physiological role in mammals altogether, but does not preclude such role e.g. in primates. Altogether, the results presented and discussed above warrant further investigations into the biological relevance of such distinct Cu(II) binding ability of human **H25**.

## CRediT authorship contribution statement

**Dawid Płonka:** Conceptualization, Investigation, Data curation, Visualization, Resources, Writing – original draft, Writing – review & editing, Funding acquisition. **Marta D. Wiśniewska:** Investigation, Data curation. **Joanna Ziemska-Legięcka:** Investigation, Data curation, Visualization, Writing – original draft. **Marcin Grynberg:** Data curation, Visualization, Writing – original draft. **Wojciech Bal:** Conceptualization, Data curation, Visualization, Resources, Writing – original draft, Writing – review & editing, Funding acquisition, Supervision, Project administration.

## Declaration of Competing Interest

The authors declare the following financial interests/personal relationships which may be considered as potential competing interests.

Member, editorial board of JIB, WB.

## Data availability

Data will be made available on request.

## Acknowledgements

This work was supported by PRELUDIUM Grant No. 2018/31/N/ST4/01259 and the OPUS Grant No. 2020/39/B/ST6/03447 (both from National Science Centre, Poland). The equipment used was sponsored in part by the Centre for Preclinical Research and Technology (CePT), a project cosponsored by the European Regional Development Fund and Innovative Economy, The National Cohesion Strategy of Poland. The graphical abstract was created with a help of Pep-Fold software [80].

## Appendix A. Supplementary data

Supplementary data to this article can be found online at https://doi.org/10.1016/j.jinorgbio.2023.112364.

## References

[1] E. Nemeth, M.S. Tuttle, J. Powelson, M.D. Vaughn, A. Donovan, D.M.V. Ward, T. Ganz, J. Kaplan, Hepcidin regulates cellular iron efflux by binding to ferroportin and inducing its internalization, Science 306 (2004) 2090–2093, https://doi.org/10.1126/science.1104742.

[2] A. Krause, S. Neitz, H.J. Mägert, A. Schulz, W.G. Forssmann, P. Schulz-Knappe, K. Adermann, LEAP-1, a novel highly disulfide-bonded human peptide, exhibits antimicrobial activity, FEBS Lett. 480 (2000) 147–150, https://doi.org/10.1016/S0014-5793(00)01920-7.

[3] H. Kulaksiz, F. Theilig, S. Bachmann, S.G. Gehrke, D. Rost, A. Janetzko, Y. Cetin, W. Stremmel, The iron-regulatory peptide hormone hepcidin: expression and cellular localization in the mammalian kidney, J. Endocrinol. 184 (2005) 361–370, https://doi.org/10.1677/joe.1.05729.

[4] C.H. Park, E.V. Valore, A.J. Waring, T. Ganz, Hepcidin, a urinary antimicrobial peptide synthesized in the liver, J. Biol. Chem. 276 (2001) 7806–7810, https://doi.org/10.1074/jbc.M008922200.

[5] H.P.E. Peters, C.M.M. Laarakkers, P. Pickkers, R. Masereeuw, O.C. Boerman, A. Eek, E.A.M. Cornelissen, D.W. Swinkels, J.F.M. Wetzels, Tubular reabsorption and local production of urine hepcidin-25, BMC Nephrol. 14 (2013) 70, https://doi.org/10.1186/1471-2369-14-70.

[6] C. Pigeon, G. Ilyin, B. Courselaud, P. Leroyer, B. Turlin, P. Brissot, O. Loréal, A new mouse liver-specific gene, encoding a protein homologous to human antimicrobial

peptide Hepcidin, is overexpressed during Iron overload, J. Biol. Chem. 276 (2001) 7811–7819, https://doi.org/10.1074/jbc.M008923200.
[7] A. Piperno, R. Mariani, P. Trombini, D. Girelli, Hepcidin modulation in human diseases: from research to clinic, World J. Gastroenterol. 15 (2009) 538–551, https://doi.org/10.3748/wjg.15.538.
[8] S. Zechel, K. Huber-Wittmer, O.B. Von Halbach, Distribution of the iron-regulating protein hepcidin in the murine central nervous system, J. Neurosci. Res. 84 (2006) 790–800, https://doi.org/10.1002/jnr.20991.
[9] S. Balesaria, B. Ramesh, H. McArdle, H.K. Bayele, S.K.S. Srai, Divalent metal-dependent regulation of hepcidin expression by MTF-1, FEBS Lett. 584 (2010) 719–725, https://doi.org/10.1016/j.febslet.2009.12.023.
[10] H. Chen, G. Huang, T. Su, H. Gao, Z.K. Attieh, A.T. McKie, G.J. Anderson, C. D. Vulpe, Decreased Hephaestin activity in the intestine of copper-deficient mice causes systemic Iron deficiency, J. Nutr. 136 (2006) 1236–1241, https://doi.org/10.1093/jn/136.5.1236.
[11] S. Jenkitkasemwong, M. Broderius, H. Nam, J.R. Prohaska, M.D. Knutson, Anemic copper-deficient rats, but not mice, display low Hepcidin expression and high Ferroportin levels, J. Nutr. 140 (2010) 723–730, https://doi.org/10.3945/JN.109.117077.
[12] T. Konz, J. Alonso-García, M. Montes-Bayón, A. Sanz-Medel, Comparison of copper labeling followed by liquid chromatography-inductively coupled plasma mass spectrometry and immunochemical assays for serum hepcidin-25 determination, Anal. Chim. Acta 799 (2013) 1–7, https://doi.org/10.1016/j.aca.2013.08.002.
[13] C. Tselepis, S.J. Ford, A.T. McKie, W. Vogel, H. Zoller, R.J. Simpson, J. Diaz Castro, T.H. Iqbal, D.G. Ward, Characterization of the transition-metal-binding properties of hepcidin, Biochem. J. 427 (2010) 289–296, https://doi.org/10.1042/BJ20091521.
[14] K. Kulprachakarn, Y.L. Chen, X. Kong, M.C. Arno, R.C. Hider, S. Srichairatanakool, S.S. Bansal, Copper(II) binding properties of hepcidin, J. Biol. Inorg. Chem. 21 (2016) 329–338, https://doi.org/10.1007/s00775-016-1342-2.
[15] A. Krężel, J. Wójcik, M. Maciejczyk, W. Bal, May GSH and L-his contribute to intracellular binding of zinc? Thermodynamic and solution structural study of a ternary complex, Chem. Commun. (2003) 704–705, https://doi.org/10.1039/B300632H.
[16] D. Płonka, R. Kotuniak, K. Dąbrowska, W. Bal, Electrospray-induced mass spectrometry is not suitable for determination of Peptidic cu(II) complexes, J. Am. Soc. Mass Spectrom. 32 (2021) 2766–2776, https://doi.org/10.1021/jasms.1c00206.
[17] P. Gonzalez, K. Bossak, E. Stefaniak, C. Hureau, L. Raibaut, W. Bal, P. Faller, N-terminal Cu-binding motifs (Xxx-Zzz-His, Xxx-His) and their derivatives: chemistry, biology and medicinal applications, Chem. - A Eur. J. 24 (2018) 8029–8041, https://doi.org/10.1002/CHEM.201705398.
[18] W. Bal, M. Jeżowska-Bojczuk, K.S. Kasprzak, Binding of nickel(II) and copper(II) to the N-terminal sequence of human protamine HP2, Chem. Res. Toxicol. 10 (1997) 906–914, https://doi.org/10.1021/tx970028x.
[19] H. Gusman, U. Lendenmann, J. Grogan, R.F. Troxler, F.G. Oppenheim, Is salivary histatin 5 a metallopeptide? Biochim. Biophys. Acta Protein Struct. Mol. Enzymol. 1545 (2001) 86–95, https://doi.org/10.1016/S0167-4838(00)00265-X.
[20] A. Kolozsi, A. Jancsó, N.V. Nagy, T. Gajda, N-terminal fragment of the anti-angiogenic human endostatin binds copper(II) with very high affinity, J. Inorg. Biochem. 103 (2009) 940–947, https://doi.org/10.1016/j.jinorgbio.2009.04.006.
[21] E. Stefaniak, D. Płonka, S.C. Drew, K. Bossak-Ahmad, K.L. Haas, M.J. Pushie, P. Faller, N.E. Wezynfeld, W. Bal, The N-terminal 14-mer model peptide of human Ctr1 can collect cu(ii) from albumin. Implications for copper uptake by Ctr1, Metallomics. 10 (2018) 1723–1727, https://doi.org/10.1039/c8mt00274f.
[22] M. Mital, N.E. Wezynfeld, T. Frączyk, M.Z. Wiloch, U.E. Wawrzyniak, A. Bonna, C. Tumpach, K.J. Barnham, C.L. Haigh, W. Bal, S.C. Drew, A functional role for Aβ in metal homeostasis? N-truncation and high-affinity copper binding, Angew. Chem. Int. Ed. 54 (2015) 10460–10464, https://doi.org/10.1002/anie.201502644.
[23] K. Stokowa-Sołtys, K. Szczerba, M. Pacewicz, R. Wieczorek, N.E. Wezynfeld, W. Bal, Interactions of neurokinin B with copper(II) ions and their potential biological consequences, Dalton Trans. 51 (2022) 14267–14276, https://doi.org/10.1039/d2dt02033e.
[24] T. Frączyk, Cu(II)-binding N-terminal sequences of human proteins, Chem. Biodivers. 18 (2021), e2100043, https://doi.org/10.1002/cbdv.202100043.
[25] S.E. Conklin, E.C. Bridgman, Q. Su, P. Riggs-Gelasco, K.L. Haas, K.J. Franz, Specific histidine residues confer Histatin peptides with copper-dependent activity against Candida albicans, Biochemistry. 56 (2017) 4244–4255, https://doi.org/10.1021/acs.biochem.7b00348.
[26] G. Domingo, L. Benussi, C. Saraceno, M. Bertuzzi, R. Nicsanu, A. Longobardi, S. Bellini, A. Cagnotto, M. Salmona, G. Binetti, R. Ghidoni, N-terminally truncated and pyroglutamate-modified Aβ forms are measurable in human cerebrospinal fluid and are potential markers of disease progression in Alzheimer's disease, Front. Neurosci. 15 (2021) 923, https://doi.org/10.3389/fnins.2021.708119.
[27] J. Kardos, L. Héja, Á. Simon, I. Jablonkai, R. Kovács, K. Jemnitz, Copper signalling: causes and consequences, Cell Commun Signal. 16 (2018) 71, https://doi.org/10.1186/s12964-018-0277-3.
[28] T. Kirsipuu, A. Zadorožnaja, J. Smirnova, M. Friedemann, T. Plitz, V. Tõugu, P. Palumaa, Copper(II)-binding equilibria in human blood, Sci. Rep. 10 (2020) 5686, https://doi.org/10.1038/s41598-020-62560-4.
[29] M.C. Linder, Apoceruloplasmin: Abundance, Detect., Format., Metabol., Biomed. 9 (2021) 233, https://doi.org/10.3390/biomedicines9030233.
[30] M.C. Linder, Ceruloplasmin and other copper binding components of blood plasma and their functions: an update, Metallomics. 8 (2016) 887–905, https://doi.org/10.1039/c6mt00103c.
[31] S. Catalani, M. Paganelli, M.E. Gilberti, L. Rozzini, F. Lanfranchi, A. Padovani, P. Apostoli, Free copper in serum: an analytical challenge and its possible applications, J. Trace Elem. Med. Biol. 45 (2018) 176–180, https://doi.org/10.1016/j.jtemb.2017.11.006.
[32] M. Moriya, Y.H. Ho, A. Grana, L. Nguyen, A. Alvarez, R. Jamil, M.L. Ackland, A. Michalczyk, P. Hamer, D. Ramos, S. Kim, J.F.B. Mercer, M.C. Linder, Copper is taken up efficiently from albumin and α2- macroglobulin by cultured human cells by more than one mechanism, Am. J. Phys. Cell Phys. 295 (2008) 708–721, https://doi.org/10.1152/ajpcell.00029.2008.
[33] J. Martinez, T.Z. Kidane, H. Tran, A. Garcia, C. Marzvaan, E. Falcone, P. Faller, M. C. Linder, Uptake of copper from hemopexin (HPX) in the absence and presence of heme by hepatic and mammary epithelial cells in culture, FASEB J. 34 (Suppl) (2020) 1, https://doi.org/10.1096/fasebj.2020.34.s1.06558.
[34] D. Bohrer, P.C. Do Nascimento, A.G. Ramirez, J.K.A. Mendonça, L.M. De Carvalho, S.C.G. Pomblum, Comparison of ultrafiltration and solid phase extraction for the separation of free and protein-bound serum copper for the Wilson's disease diagnosis, Clin. Chim. Acta 345 (2004) 113–121, https://doi.org/10.1016/j.cccn.2004.03.001.
[35] D.J. Frommer, Direct measurement of serum non-caeruloplasmin copper in liver disease, Clin. Chim. Acta 68 (1976) 303–307, https://doi.org/10.1016/0009-8981(76)90395-8.
[36] G.A. McMillin, J.J. Travis, J.W. Hunt, Direct measurement of free copper in serum or plasma ultrafiltrate, Am. J. Clin. Pathol. 131 (2009) 160–165, https://doi.org/10.1309/AJCP7Z9KBFINVGYF.
[37] E. Falcone, M. Okafor, N. Vitale, L. Raibaut, A. Sour, P. Faller, Extracellular Cu2+ pools and their detection: from current knowledge to next-generation probes, Coord. Chem. Rev. 433 (2021), 213727, https://doi.org/10.1016/j.ccr.2020.213727.
[38] K. Bossak-Ahmad, T. Frączyk, W. Bal, S.C. Drew, The sub-picomolar Cu2+ dissociation constant of human serum albumin, ChemBioChem. 21 (2020) 331–334, https://doi.org/10.1002/cbic.201900435.
[39] S. Yoshino, K. Fujimoto, T. Takada, S. Kawamura, J. Ogawa, Y. Kamata, Y. Kodera, M. Shichiri, Molecular form and concentration of serum α2-macroglobulin in diabetes, Sci. Report. 91 (9) (2019) 1–10, https://doi.org/10.1038/s41598-019-49144-7.
[40] A. Garcia, D. Ramos, C. Marzvaan, B. Vileno, P. Faller, M.C. Linder, Comparison of Alpha-2-macroglobulins from swine and humans and their copper binding, FASEB J. 33 (2019), https://doi.org/10.1096/fasebj.2019.33.1_supplement.825.3, 825.3.
[41] L. Jiang, M.D. Garrick, L.M. Garrick, L. Zhao, J.F. Collins, Divalent metal transporter 1 (Dmt1) mediates copper transport in the duodenum of Iron-deficient rats and when overexpressed in Iron-deprived HEK-293 cells, J. Nutr. 143 (2013) 1927–1933, https://doi.org/10.3945/JN.113.181867.
[42] C. Lin, Z. Zhang, T. Wang, C. Chen, Y. James Kang, Copper uptake by DMT1: A compensatory mechanism for CTR1 deficiency in human umbilical vein endothelial cells, Metallomics. 7 (2015) 1285–1289, https://doi.org/10.1039/c5mt00097a.
[43] C. Doguer, J.H. Ha, J.F. Collins, Intersection of Iron and copper metabolism in the mammalian intestine and liver, Compr. Physiol. 8 (2018) 1433–1461, https://doi.org/10.1002/cphy.c170045.
[44] Y.A. Seo, J.A. Elkhader, M. Wessling-Resnick, Distribution of manganese and other biometals in flatiron mice, BioMetals. 29 (2016) 147–155, https://doi.org/10.1007/s10534-015-9904-2.
[45] D. Płonka, W. Bal, The N-terminus of hepcidin is a strong and potentially biologically relevant cu(II) chelator, Inorg. Chim. Acta 472 (2018) 76–81, https://doi.org/10.1016/j.ica.2017.06.051.
[46] T. Konz, M. Montes-Bayón, A. Sanz-Medel, Elemental labeling and isotope dilution analysis for the quantification of the peptide hepcidin-25 in serum samples by HPLC-ICP-MS, Anal. Chem. 84 (2012) 8133–8139, https://doi.org/10.1021/ac300578n.
[47] M. Sokolowska, A. Krezel, M. Dyba, Z. Szewczuk, W. Bal, Short peptides are not reliable models of thermodynamic and kinetic properties of the N-terminal metal binding site in serum albumin, Eur. J. Biochem. 269 (2002) 1323–1331, https://doi.org/10.1046/j.1432-1033.2002.02772.x.
[48] I. Zawisza, M. Rózga, W. Bal, Affinity of copper and zinc ions to proteins and peptides related to neurodegenerative conditions (Aβ, APP, α-synuclein, PrP), Coord. Chem. Rev. 256 (2012) 2297–2307, https://doi.org/10.1016/j.ccr.2012.03.012.
[49] R.C. Chen, C.Y. Lan, Human antimicrobial peptide hepcidin 25-induced apoptosis in candida albicans, Microorganisms. 8 (2020) 585, https://doi.org/10.3390/microorganisms8040585.
[50] W. Chan, P. White, Fmoc Solid Phase Peptide Synthesis. Practical Approach, Oxford University Press, Oxford, 1999. http://www.worldcat.org/oclc/1027202119.
[51] J. Zhang, S. Diamond, T. Arvedson, B.J. Sasu, L.P. Miranda, Oxidative folding of hepcidin at acidic pH, Biopolymers. 94 (2010) 257–264, https://doi.org/10.1002/bip.21383.
[52] J.B. Jordan, L. Poppe, M. Haniu, T. Arvedson, R. Syed, V. Li, H. Kohno, H. Kim, P. D. Schnier, T.S. Harvey, L.P. Miranda, J. Cheetham, B.J. Sasu, Hepcidin revisited, disulfide connectivity, dynamics, and structure, J. Biol. Chem. 284 (2009) 24155–24167, https://doi.org/10.1074/jbc.M109.017764.
[53] P. Gans, A. Sabatini, A. Vacca, SUPERQUAD: an improved general program for computation of formation constants from potentiometric data, J. Chem. Soc. Dalton Trans. (1985) 1195–1200, https://doi.org/10.1039/DT9850001195.
[54] P. Gans, A. Sabatini, A. Vacca, Investigation of equilibria in solution. Determination of equilibrium constants with the HYPERQUAD suite of programs, Talanta. 43 (1996) 1739–1753, https://doi.org/10.1016/0039-9140(96)01958-3.

[55] M. Scarpa, F. Vianello, L. Signor, L. Zennaro, A. Rigo, Ascorbate oxidation catalyzed by Bis(histidine)copper(II), Inorg. Chem. 35 (1996) 5201–5206, https://doi.org/10.1021/ic9600644.
[56] M. Sokołowska, W. Bal, Cu(II) complexation by "non-coordinating" N-2-hydroxyethylpiperazine-N′-2-ethanesulfonic acid (HEPES buffer), J. Inorg. Biochem. 99 (2005) 1653–1660, https://doi.org/10.1016/j.jinorgbio.2005.05.007.
[57] L.S. Johnson, S.R. Eddy, E. Portugaly, Hidden Markov model speed heuristic and iterative HMM search procedure, BMC Bioinform. 11 (2010) 431, https://doi.org/10.1186/1471-2105-11-431.
[58] S.C. Potter, A. Luciani, S.R. Eddy, Y. Park, R. Lopez, R.D. Finn, HMMER web server: 2018 update, Nucleic Acids Res. 46 (2018) W200–W204, https://doi.org/10.1093/nar/gky448.
[59] A. Bateman, M.J. Martin, S. Orchard, M. Magrane, R. Agivetova, S. Ahmad, E. Alpi, E.H. Bowler-Barnett, R. Britto, B. Bursteinas, H. Bye-A-Jee, R. Coetzee, A. Cukura, A. da Silva, P. Denny, T. Dogan, T.G. Ebenezer, J. Fan, L.G. Castro, P. Garmiri, G. Georghiou, L. Gonzales, E. Hatton-Ellis, A. Hussein, A. Ignatchenko, G. Insana, R. Ishtiaq, P. Jokinen, V. Joshi, D. Jyothi, A. Lock, R. Lopez, A. Luciani, J. Luo, Y. Lussi, A. MacDougall, F. Madeira, M. Mahmoudy, M. Menchi, A. Mishra, K. Moulang, A. Nightingale, C.S. Oliveira, S. Pundir, G. Qi, S. Raj, D. Rice, M. R. Lopez, R. Saidi, J. Sampson, T. Sawford, E. Speretta, E. Turner, N. Tyagi, P. Vasudev, V. Volynkin, K. Warner, X. Watkins, R. Zaru, H. Zellner, A. Bridge, S. Poux, N. Redaschi, L. Aimo, G. Argoud-Puy, A. Auchincloss, K. Axelsen, P. Bansal, D. Baratin, M.C. Blatter, J. Bolleman, E. Boutet, L. Breuza, C. Casals-Casas, E. de Castro, K.C. Echioukh, E. Coudert, B. Cuche, M. Doche, D. Dornevil, A. Estreicher, M.L. Famiglietti, M. Feuermann, E. Gasteiger, S. Gehant, V. Gerritsen, A. Gos, N. Gruaz-Gumowski, U. Hinz, C. Hulo, N. Hyka-Nouspikel, F. Jungo, G. Keller, A. Kerhornou, V. Lara, P. Le Mercier, D. Lieberherr, T. Lombardot, X. Martin, P. Masson, A. Morgat, T.B. Neto, S. Paesano, I. Pedruzzi, S. Pilbout, L. Pourcel, M. Pozzato, M. Pruess, C. Rivoire, C. Sigrist, K. Sonesson, A. Stutz, S. Sundaram, M. Tognolli, L. Verbregue, C.H. Wu, C.N. Arighi, L. Arminski, C. Chen, Y. Chen, J.S. Garavelli, H. Huang, K. Laiho, P. McGarvey, D. A. Natale, K. Ross, C.R. Vinayaka, Q. Wang, Y. Wang, L.S. Yeh, J. Zhang, P. Ruch, D. Teodoro, UniProt: the universal protein knowledgebase in 2021, Nucleic Acids Res. 49 (2021) D480–D489, https://doi.org/10.1093/nar/gkaa1100.
[60] N.A. O'Leary, M.W. Wright, J.R. Brister, S. Ciufo, D. Haddad, R. McVeigh, B. Rajput, B. Robbertse, B. Smith-White, D. Ako-Adjei, A. Astashyn, A. Badretdin, Y. Bao, O. Blinkova, V. Brover, V. Chetvernin, J. Choi, E. Cox, O. Ermolaeva, C. M. Farrell, T. Goldfarb, T. Gupta, D. Haft, E. Hatcher, W. Hlavina, V.S. Joardar, V. K. Kodali, W. Li, D. Maglott, P. Masterson, K.M. McGarvey, M.R. Murphy, K. O'Neill, S. Pujar, S.H. Rangwala, D. Rausch, L.D. Riddick, C. Schoch, A. Shkeda, S.S. Storz, H. Sun, F. Thibaud-Nissen, I. Tolstoy, R.E. Tully, A.R. Vatsan, C. Wallin, D. Webb, W. Wu, M.J. Landrum, A. Kimchi, T. Tatusova, M. DiCuccio, P. Kitts, T. D. Murphy, K.D. Pruitt, Reference sequence (RefSeq) database at NCBI: current status, taxonomic expansion, and functional annotation, Nucleic Acids Res. 44 (2016) D733–D745, https://doi.org/10.1093/nar/gkv1189.
[61] J. Huerta-Cepas, F. Serra, P. Bork, ETE 3: reconstruction, analysis, and visualization of Phylogenomic data, Mol. Biol. Evol. 33 (2016) 1635–1638, https://doi.org/10.1093/molbev/msw046.
[62] I.M. Abbas, M. Vranic, H. Hoffmann, A.H. El-Khatib, M. Montes-Bayón, H. M. Möller, M.G. Weller, Investigations of the copper peptide hepcidin-25 by LC-MS/MS and NMR+, Int. J. Mol. Sci. 19 (2018) 2271, https://doi.org/10.3390/ijms19082271.
[63] G. Krainer, S. Keller, Single-experiment displacement assay for quantifying high-affinity binding by isothermal titration calorimetry, Methods. 76 (2015) 116–123, https://doi.org/10.1016/j.ymeth.2014.10.034.
[64] M. Jerabek-Willemsen, T. André, R. Wanner, H.M. Roth, S. Duhr, P. Baaske, D. Breitsprecher, MicroScale thermophoresis: interaction analysis and beyond, J. Mol. Struct. 1077 (2014) 101–113, https://doi.org/10.1016/j.molstruc.2014.03.009.
[65] M. Mital, K. Szutkowski, K. Bossak-Ahmad, P. Skrobecki, S.C. Drew, J. Poznański, I. Zhukov, T. Frączyk, W. Bal, The palladium(II) complex of $A\beta_{4-16}$ as suitable model for structural studies of biorelevant copper(ii) complexes of N-truncated beta-amyloids, Int. J. Mol. Sci. 21 (2020) 9200, https://doi.org/10.3390/ijms21239200.
[66] A. Santoro, G. Walke, B. Vileno, P.P. Kulkarni, L. Raibaut, P. Faller, Low catalytic activity of the cu(II)-binding motif (Xxx-Zzz-His; ATCUN) in reactive oxygen species production and inhibition by the cu(i)-chelator BCS, Chem. Commun. 54 (2018) 11945–11948, https://doi.org/10.1039/c8cc06040a.
[67] K.B. Hilton, L.A. Lambert, Molecular evolution and characterization of hepcidin gene products in vertebrates, Gene. 415 (2008) 40–48, https://doi.org/10.1016/j.gene.2008.02.016.
[68] R.J. Clark, C.C. Tan, G.C. Preza, E. Nemeth, T. Ganz, D.J. Craik, Understanding the structure/activity relationships of the iron regulatory peptide hepcidin, Chem. Biol. 18 (2011) 336–343, https://doi.org/10.1016/j.chembiol.2010.12.009.
[69] G. Maisetta, R. Petruzzelli, F.L. Brancatisano, S. Esin, A. Vitali, M. Campa, G. Batoni, Antimicrobial activity of human hepcidin 20 and 25 against clinically relevant bacterial strains: effect of copper and acidic pH, Peptides. 31 (2010) 1995–2002, https://doi.org/10.1016/j.peptides.2010.08.007.
[70] R. Kotuniak, M.J.F. Strampraad, K. Bossak-Ahmad, U.E. Wawrzyniak, I. Ufnalska, P.L. Hagedoorn, W. Bal, Key intermediate species reveal the copper(II)-exchange pathway in biorelevant ATCUN/NTS complexes, Angew. Chem. Int. Ed. 59 (2020) 11234–11239, https://doi.org/10.1002/anie.202004264.
[71] J. Portelinha, S.S. Duay, S.I. Yu, K. Heilemann, M.D.J. Libardo, S.A. Juliano, J. L. Klassen, A.M. Angeles-Boza, Antimicrobial peptides and copper(II) ions: novel therapeutic opportunities, Chem. Rev. 121 (2021) 2648–2712, https://doi.org/10.1021/acs.chemrev.0c00921.
[72] T. Ganz, G. Olbina, D. Girelli, E. Nemeth, M. Westerman, Immunoassay for human serum hepcidin, Blood. 112 (2008) 4292–4297, https://doi.org/10.1182/blood-2008-02-139915.
[73] T.E. Galesloot, S.H. Vermeulen, A.J. Geurts-Moespot, S.M. Klaver, J.J. Kroot, D. Van Tienoven, J.F.M. Wetzels, L.A.L.M. Kiemeney, F.C. Sweep, M. Den Heijer, D. W. Swinkels, Serum hepcidin: reference ranges and biochemical correlates in the general population, Blood. 117 (2011) e218–e225, https://doi.org/10.1182/blood-2011-02-337907.
[74] G. Fanali, A. Di Masi, V. Trezza, M. Marino, M. Fasano, P. Ascenzi, Human serum albumin: from bench to bedside, Mol. Asp. Med. 33 (2012) 209–290, https://doi.org/10.1016/j.mam.2011.12.002.
[75] J.J. Xiao, W. Krzyzanski, Y.M. Wang, H. Li, M.J. Rose, M. Ma, Y. Wu, B. Hinkle, J. J. Perez-Ruixo, Pharmacokinetics of anti-hepcidin monoclonal antibody ab 12B9m and hepcidin in cynomolgus monkeys, AAPS J. 12 (2010) 646–657, https://doi.org/10.1208/s12248-010-9222-0.
[76] R. Kotuniak, W. Bal, Kinetics of Cu(ii) complexation by ATCUN/NTS and related peptides: a gold mine of novel ideas for copper biology, Dalton Trans. 51 (2022) 14–26, https://doi.org/10.1039/d1dt02878b.
[77] R. Kotuniak, W. Bal, Reactive Cu2+−peptide intermediates revealed by kinetic studies gain relevance by matching time windows in copper metallomics, Metallomics 15 (2023) mfad007, https://doi.org/10.1093/mtomcs/mfad007.
[78] G. Peslova, J. Petrak, K. Kuzelova, I. Hrdy, P. Halada, P.W. Kuchel, S. Soe-Lin, P. Ponka, R. Sutak, E. Becker, M.L.H. Huang, Y.S. Rahmanto, D.R. Richardson, D. Vyoral, Hepcidin, the hormone of iron metabolism, is bound specifically to α-2-macroglobulin in blood, Blood. 113 (2009) 6225–6236, https://doi.org/10.1182/blood-2009-01-201590.
[79] O. Itkonen, U.H. Stenman, J. Parkkinen, R. Soliymani, M. Baumann, E. Hamäläinen, Binding of hepcidin to plasma proteins, Clin. Chem. 58 (2012) 1158–1160, https://doi.org/10.1373/clinchem.2012.186916.
[80] P. Thévenet, Y. Shen, J. Maupetit, F. Guyon, P. Derreumaux, P. Tufféry, PEP-FOLD: an updated de novo structure prediction server for both linear and disulfide bonded cyclic peptides, Nucleic Acids Res 40 (2012) W288–W293, https://doi.org/10.1093/nar/gks419.